

Numerical modelling of dual point contact induced ultrasonic waves in PZT ceramics

V. Agarwal¹, A. Habib², B. S. Ahluwalia², F. Melandsø², and A. Shelke¹

¹Department of Civil Engineering, Indian Institute of Technology Guwahati, Assam 781039, India

²Department of Physics and Technology, UiT The Arctic University of Norway, Norway

1. Introduction

Piezoelectric materials such as Lead zirconate titanate $Pb(Zr_xTi_{1-x})O_3$ (PZT) have found widespread use as reliant electromechanical sensors and actuators. Manufacturing and applications of PZT have developed rapidly over the years because of its small volume, lightweight, efficient conversions between mechanical and electrical energy and wide bandwidth¹. Numerous studies have already been performed in the last several decades in order to characterize and optimize its piezoelectric properties².

PZT found its use in the field of ultrasonic imaging because of higher electromechanical coupling than the conventional piezoelectric materials and appropriate acoustic impedance^{3, 4}. Though PZT ceramics were extensively used in ultrasonic imaging of other medical and engineering samples, but very few studies were conducted to determine the internal response of PZT that were electrically or mechanically actuated. Moreover, numerical modelling of PZT ceramics to observe this internal response is not yet available in the literature.

Recently, the propagation of ultrasonic waves in PZT ceramic was experimentally visualized using scanned Coulomb coupling method⁵. This also broadened the domain of ultrasonic imaging of not only on PZT ceramics but also in other piezoelectric materials⁶⁻⁸. The main objective of this study is to model numerically the response of the PZT ceramics employing a dual point contact excitation and detection method. In the same time, scattering and attenuation of the ultrasonic waves have been observed due to artificial defect into the PZT ceramics. This study adopts the finite element analysis (FEM) method to access the dynamics of PZT ceramics since it has the ability to solve the complete set of fundamental equations for a 3-D model⁹.

email: Vikram.2015@iitg.ac.in

2. FEM Study using COMSOL

A profound study of the mechanics of wave propagation in PZT solids is implemented with the support of COMSOL 5.2. Practical transducers often require a full 3-D representation to replicate any numerical model⁹. Thus an analysis system has been implemented with no restraint other than linearity. A point on the top surface of the PZT is charged with a Dirac-delta pulse with a duration of 75 ns and the other surface of the ceramic is considered grounded. Later on, a cylindrical hollow damage is modelled on the surface of the PZT with a radius of $\lambda/10$ Where, λ is the wavelength of the input pulse. The PZT ceramic is meshed with tetrahedral blocks with a maximum element size of $\lambda/20$. A time-dependent study is then carried out at a time increment of T. Where T is the time period of the delta pulse.

3. Equations Governing Piezoelectric Behaviour

The strain-charge form of piezoelectric constitutive equations is given by¹⁰:

$$S = s^E T + dE \quad (1)$$

$$D = \varepsilon^T E + dT \quad (2)$$

Where S : Mechanical strain vector, s^E : Elastic compliance tensor (Pa^{-1}), T : Mechanical stress vector (Nm^{-2}), d : Electro-mechanical coupling factor (CN^{-1}), E : Electric field vector (Vm^{-1}), D : Electrical displacement (Cm^{-2}), ε^T : Dielectric permittivity tensor (Fm^{-1}). Electrical response in the PZT ceramics can be determined using Gauss law, which relates electric displacement with the free electric charge density.

$$\nabla \cdot D = \rho_f \quad (3)$$

The total free charge accumulated in the entire PZT crystal Volume (V) is given by:

$$Q_f = \int_{vol} \rho_f dV \quad (4)$$

The capacitance of the PZT ceramics and the voltage produced by its electrodes are:

$$C_p = \frac{eA_p}{t_p} \quad (5)$$

$$V_p = \frac{Q_f}{C_p} \quad (6)$$

Where e is the electric permittivity, A_p is the area and t_p is the thickness of the PZT crystal.

4. Simulation Results

The typical normalized voltage response at a point on the top surface of PZT is shown in fig.1.

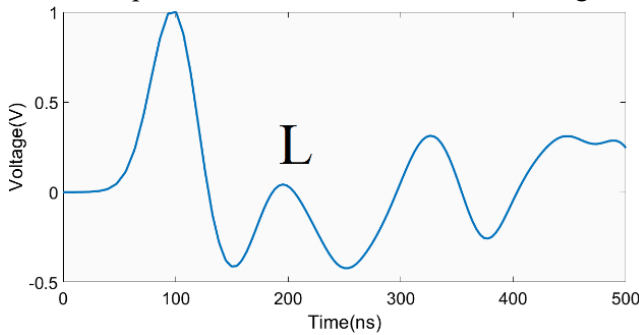


Fig.1 Normalised transient voltage signal obtained at a point on the surface of PZT ceramic with L indicating the first longitudinal wave

The first peak indicates the excitation signal and is observed around 100 ns. The second wave arrives at 195 ± 15 ns and designates the first longitudinal bulk wave. Fig. 2 shows the time sequential images indicating the evolution of acoustic waves in the PZT ceramic.

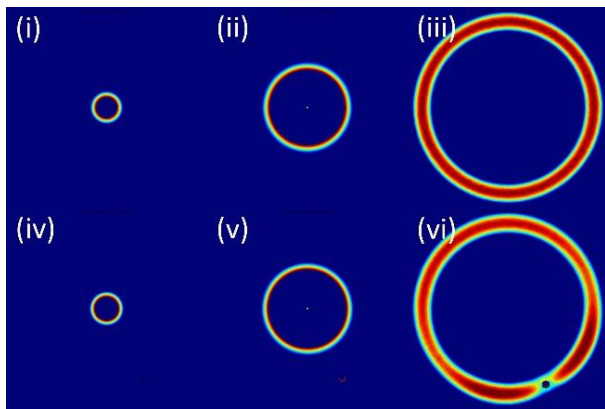


Fig. 2 : Sequential images of healthy (i) to (iii) and damage state (iv) to (vi) of the top surface of PZT ceramic

In fig (i) to (iii) it can be observed that the PZT ceramic is homogeneous and isotropic regarding the

transport properties of acoustic waves. The effect of localised defect in the PZT ceramic can be observed in fig 2 (iv) to (vi). The attenuation and scattering of acoustic waves in damage case is clearly visible in fig 2 (vi). The calculated bulk longitudinal velocity in the PZT ceramic was 4220 m/s.

5. Conclusion

A 3-D numerical simulation of PZT ceramic using COMSOL Multiphysics has been successfully conducted. The waves propagation inside the PZT ceramic due to point contact excitation is presented. Scattering and attenuation of the ultrasonic waves due to the presence of a surface defect. This study adds to the existing knowledge of the internal response of PZT ceramics when excited with dual point contact induced ultrasonic waves. Future perspective in this domain of engineering can be seen in the use of such simulations for structural health monitoring of piezoelectric ceramics.

Acknowledgement

This work was supported by SIUGC funded INCP project (2014/10024).

References

1. X. J. Dong, G. Meng and J.-C. Peng: J. Sound Vib. **297** (2006) 680.
2. J. Carrano, C. Sudhama, V. Chikarmane, J. Lee, A. Tasch, W. Shepherd and N. Abt: IEEE Trans. Ultrason. Ferroelectr. Freq. Control. **38** (1991) 690.
3. S. E. Park and T.R. Shrout: IEEE Trans. Ultrason. Ferroelectr. Freq. Control. **44** (1997) 1140.
4. W. A. Smith: Applications of Ferroelectrics. 6th IEEE Int. Symp.1986, p. 249.
5. A. Habib, A. Shelke, M. Pluta, T. Kundu, U. Pietsch and W. Grill: Jpn. J. Appl. Phys., **51** (2012) 07GB05.
6. A. Habib, U. Amjad, M. Pluta, U. Pietsch and W. Grill: in SPIE, San Diego, 2010, p. 76501T.
7. A. Habib, E. Twerdowski, M. von Buttlar, M. Pluta, M. Schmachtl, R. Wannemacher and W. Grill:, 2006, p. 61771A.
8. A. Habib, A. Shelke, M. Pluta, U. Pietsch, T. Kundu and W. Grill: AIP Conf. Proce., 2012, p. 247.
9. R. Lerch: IEEE Trans. Ultrason. Ferroelectr. Freq. Control. **37** (1990) 233.
10. T. Meeker: IEEE Trans. Ultrason. Ferroelectr. Freq. Control. **43** (1996) 717.